

Towards Completing a Large Area ULIRG Survey [★]

D.L. Clements,^{1,2} W.J. Saunders³ and R.G. McMahon⁴

¹*European Southern Observatory, Karl-Schwarzschild-Strasse 2, D-85748 Garching-bei-Munchen, Germany*

²*IAS, Batiment 121, Universite Paris XI, 91045 ORSAY Cedex, France*

³*Institute for Astronomy, Edinburgh University, ROE, Blackford Hill, Edinburgh*

⁴*Institute of Astronomy, Madingley Road, Cambridge*

12 April 2017

ABSTRACT

We present the latest results in our efforts to produce a complete, large sample of Ultraluminous Infrared Galaxies (ULIRGs, $L_{60} > 10^{11.4} L_{\odot}$ for $H_0 = 100 \text{ km s}^{-1} \text{ Mpc}^{-1}$, $q_0 = 0.5$) for use in the study of these objects and their evolution. We have been using an optical/IR colour technique to select those objects most likely to be ULIRGs. 65 of the 198 candidate ULIRGs that do not yet have redshifts were observed. Redshifts were obtained for 51 of these objects, including 8 new ULIRGs and a further three probable ULIRGs with tentative redshifts. The new ULIRGs include one object at $z = 0.44$ (00029-1424), the highest in the survey so far, and at least one new broad-line ULIRG (03156-1706) which appears to lie in a galaxy cluster. We discuss the properties of these objects and their local environments, concluding that three of them have high excitation spectra, and that five show disturbed morphology even in the shallow acquisition images. We also present the redshift measurements of the non-ULIRGs identified in the course of this survey.

Key words: infrared;galaxies – galaxies;starburst – galaxies;interacting – galaxies;specific;00029-1424 – galaxies;specific;03156-1706

1 INTRODUCTION

One of the most spectacular results of the IRAS satellite survey was the discovery of galaxies with huge luminosities in the far-infrared (far-IR, $\approx 8 - 1000 \mu\text{m}$) (e.g Wright et al, 1984). The far-IR luminosity of these objects typically exceeds their optical and UV luminosity by factors of 2 - 80 (see Sanders & Mirabel, 1996 and references therein). These far-IR galaxies are relatively common in the nearby Universe; at lower luminosities ($10^{9.4} - 10^{10.4} L_{\odot}$ $H_0 = 100 \text{ km s}^{-1} \text{ Mpc}^{-1}$) their space density is comparable with that of Markarian starbursts, whilst at the highest luminosities, $> 10^{11.4} L_{\odot}$, they are roughly as common as quasars of similar power output (Sanders et al 1989, Rowan-Robinson 1995). Objects this powerful have been termed ultraluminous infrared galaxies, ULIRGs.

There are many unanswered questions regarding these ULIRGs. It is still unclear just what powers their far-IR emission, especially at the highest luminosities, or what evolutionary role they play in the development of galaxies. Recent results from ISO are suggesting that starbursts, rather than AGN, may dominate their luminosity (Lutz et al 1996),

but this issue is still far from settled (see eg. Lonsdale et al. 1998).

One of the main obstacles to our understanding of ULIRGs is the small number so far uncovered in the IRAS source catalogues. For example, only 3 % of the IRAS Bright Galaxy Sample (Sanders et al 1988) had luminosities $> 10^{11.4} L_{\odot}$, the defining characteristic of a ULIRG for our assumed value of H_0 . The 10 ULIRGs discovered in the BGS are the best studied of this class of object, but it is only with larger samples that we may perform the statistical studies necessary to reveal their range of properties and their true evolutionary role in the universe. Of the 10 BGS ULIRGs, 9 possess high ionization spectra, typical of objects powered by an active nucleus, and all 10 seem to be merging or interacting systems (Sanders et al 1988). On this basis it has been suggested that ULIRGs are an early stage in the development of quasars.

Larger flux limited surveys of IRAS galaxies, and lists of ULIRGs discovered as a result, are gradually becoming available. Recent work includes Kim et al. (1995) and Veilleux et al. (1995), which includes extensive analysis of both nuclear and off-nuclear spectroscopy, and Fisher et al. (1995). Other ULIRG surveys are discussed in Sanders and Mirabel (1996) and in Clements et al. (1996a, hereinafter Paper 1, and 1996b).

[★] Based on observations collected at the European Southern Observatory, La Silla, Chile

The evolutionary role of ULIRGs is also of great interest. It is still unclear whether the rapid evolution of IRAS galaxies (e.g. Saunders et al. 1990) parallels the density evolution of the faint blue population (Broadhurst et al. 1988, Colless et al. 1990) or the luminosity evolution of radio galaxies and quasars (Boyle et al. 1988; Dunlop & Peacock, 1990). Samples of IRAS galaxies based on the IRAS Point Source Catalogue (PSC) contain too few galaxies at cosmologically significant redshifts to distinguish between the two types of evolution. Selection from the deeper Faint Source Survey may be able to reach the necessary depths. We have thus been conducting a programme to identify candidate ULIRGs over a large region of sky (~ 0.7 steradians) using the Faint Source Survey to reach a limiting flux of 0.3 Jy at $60\mu\text{m}$. The first results from this survey programme were discussed in Paper 1. That paper provided basic data on 91 ULIRGs found in our survey region. The present paper presents the results of further spectroscopy of candidate ULIRGs in the same area, including the discovery of 11 new or probable ULIRGs.

The rest of this paper is organised as follows. In the next section we briefly review the selection techniques for our survey. In section 3 we describe the observations and data reduction. Our results are presented in Section 4, while in section 5 we discuss these results and the current status of the survey. In section 6 we draw our conclusions.

We assume $H_0 = 100 \text{ km s}^{-1} \text{ Mpc}^{-1}$ and $q_0 = 0.5$ throughout.

2 SAMPLE SELECTION

The targets for the present observations are all part of the large ULIRG survey first described in Paper 1. A detailed description of our selection techniques can be found there, but we include a brief summary here.

The basic data for the survey is the IRAS Faint Source Survey V1.2 (Moshir et al. 1992) and UK Schmidt Telescope survey plates covering the region $b < 50^\circ$ and $-32.5^\circ < \text{DEC} < +2.5^\circ$. IRAS sources with galaxy-like colours were identified with optical counterparts on the scanned plates using a maximum likelihood technique (Sutherland & Saunders, 1992; Paper 1). To select ULIRG candidates from this list, we then examine the optical/far-IR flux ratio. It has been found that the optical galaxy luminosity function has a rather sharp cut-off at high luminosities, with almost no galaxy having $L_{\lambda} \gtrsim 4 \times 10^{10} L_{B\odot}$. The Far-IR luminosity function, in contrast, has no such cut-off. Any galaxy with an extreme IR luminosity will thus have a large ratio of optical to infrared flux, $\gtrsim 20$.

We thus define:

$$R_1 = f_{60} \text{dex}[0.4(B_J - 14.45)] = \frac{f_{60}}{f_B} \quad (1)$$

$$R_2 = R_1 \frac{f_{60}}{\max(f_{100}, f_{60})} \quad (2)$$

and select sources with either R_1 or $R_2 > 10$ as candidate ULIRGs.

There are 479 sources that meet this criterion and are above our adopted $60\mu\text{m}$ flux limit of 0.3 Jy in our survey area. Literature searches and the observations described in Paper 1 have identified 278 of these sources as galaxies and

a further 3 as stars. Of the 278 galaxies, 91 turned out to be ULIRGs, suggesting that we have a $\sim 33\%$ success rate for finding ULIRGs with this technique. This contrasts very well with the $\sim 3\%$ of IRAS sources found to be ULIRGs in simple flux limited samples. The observational targets for the present paper have been selected from the remaining 198 sources that have yet to have redshifts measured.

3 OBSERVATIONS AND DATA REDUCTION

The observations were carried out on the ESO 3.6m telescope using the EFOSC1 instrument on the nights of 29 – 31st July 1995. The EFOSC1 instrument uses a 512 by 512 Tektronix CCD and can provide both imaging observations and, via a slit and grism, spectroscopy (Melnick, 1995). For the present observations, acquisition images were made using the standard R band filter, and spectroscopy was obtained using the R300 grism. This provides a spectral range of $5940 - 9770\text{\AA}$. The resolution was measured using the arc lamp to be 16.5\AA . In imaging mode, the plate scale is 0.6 arcseconds per pixel. Acquisition images were typically 120s long, while spectra received typical integration times of 300s.

The data were reduced in the usual way using the IRAF system. Bias frames were subtracted and then the images were flat fielded, using sky flats for images and dome flats for the spectra. Spectra were wavelength calibrated using a Helium-Argon arc lamp. Conditions were generally non-photometric and with seeing ranging from 1 to 2 arcseconds. The spectroscopic standard LTT7379 was used to flatten the CCD response function and to provide some correction for the A and B atmospheric absorption bands.

The most prominent line in almost all ULIRG optical spectra is usually the $\text{H}\alpha 6563 + \text{NII} 6548/6583$ doublet blend. In many cases only this line and the $\text{SII} 6716/6731$ doublet are detected, since strong dust absorption in these objects suppresses emission lines at shorter wavelengths. The redshifts for these objects are thus generally calculated from these two emission lines only, using Gaussian fits to the lines. The resolution of the observations are not quite high enough to allow a full deconvolution of the $\text{H}\alpha$ -NII blend, but they are high enough to allow an estimate to be made of the relative strengths of the $\text{H}\alpha$ and NII lines in some cases. If NII emission is stronger than $\text{H}\alpha$, we classify the object as having a high excitation spectrum, usually Seyfert 2 or LINER-like. A high excitation spectrum can indicate objects containing an active nucleus. Our previous observations (Paper 1) using FOSII at the WHT with a resolution of 25\AA could not achieve this.

4 RESULTS

Of the 65 objects observed, redshifts were obtained for 51, including 11 new or probable ULIRGs. Five proved to be stars and 6 had featureless spectra. Table 1 presents the basic parameters for the new ULIRGs discovered in this work, while Appendix A provides information for the non-ULIRG IRAS galaxies that we have identified. Figure 1 presents the spectra for the new ULIRGs, while Figure 2 presents their images.

Name	RA(1950)	DEC(1950)	F ₆₀ (Jy)	z	log(L ₆₀ (L _⊙))
00029-1424	00 02 56.8	-14 24 26.0	0.37	0.440	12.08
00285-3140	00 28 34.7	-31 40 52.0	0.39	0.219*	11.46
00366-0503	00 36 38.6	-05 03 55.0	0.43	0.40*	12.04
00415-0737	00 41 33.5	-07 37 38.0	0.40	0.312	11.79
00482-2720	00 48 13.9	-27 20 60.0	1.13	0.129	11.45
01098-2754	01 09 53.8	-27 54 17.6	0.64	0.220	11.68
02226-1658	02 22 36.3	-16 58 26.0	0.53	0.233*	11.65
03156-1706	03 15 40.9	-17 06 02.0	0.34	0.351	11.83
21498-2636	21 49 49.1	-26 36 12.7	0.33	0.243	11.48
23169-0818	23 16 59.3	-08 18 46.0	0.34	0.248	11.51
23569-0341	23 56 59.8	-03 41 55.0	0.35	0.304	11.71

Table 1. Table of newly discovered ULIRGs. Asterisks indicate tentative redshifts based on single emission lines.

4.1 Notes on Specific Objects

We here include details on both the spectrum and image of each of the new ULIRGs.

00029-1424 A somewhat broad line is detected and identified with H α at $z=0.44$. There are no matching atmospheric features at this wavelength so we believe it to be a secure detection. A second line is marginally detected at a wavelength matching SII at the same redshift. The velocity width of the H α line is $\sim 2000 \text{ kms}^{-1}$, so we tentatively identify this object as an AGN.

The optical image of this ULIRG is a barely resolved faint source. No morphological classification is possible.

00285-3140 A line is detected at 7986\AA which we tentatively identify as the H α -NII blend. We can say nothing about the nature of this object given the scant information in the spectrum. The identification as a ULIRG, must be regarded as tentative since only a single line is detected.

The image of this object is barely resolved. No morphological assessment can be made.

00366-0503 We tentatively identify a feature in the spectrum of this object at 9175\AA with the H α -NII blend. This line is not associated with any atmospheric features, unlike the one at $\sim 8800\text{\AA}$. This places the object at $z=0.4$, though this redshift must be regarded as tentative until further confirmation can be obtained. It is interesting to note that the spectrum for this object is quite blue, unlike most others in the present paper.

This ULIRG is barely resolved in the optical image. No morphological assessment is possible.

00415-0737 The H α -NII blend is clearly detected in this object, along with SII. The NII emission appears to be very strong, indicating a likely high excitation spectrum. There is also a marginal detection of the OIII5007/4959 doublet, but no sign of H β , giving $\log(\text{OIII}/\text{H}\beta) > 0.6$ which suggests an AGN-like ionising spectrum (see Paper 1).

The image of this galaxy shows a distinct plume or extension to the SE, suggesting that it is a disturbed system.

00482-2720 H α is strongly detected in this galaxy, and marginally resolved from the NII lines. SII is also detected, but is partially suppressed by the atmospheric A band at 7700\AA . OI6300 is also detected. On the basis of the marginally resolved H α -NII blend, this galaxy is classified as HII region-like.

This galaxy has a second nucleus or plume to the SW and a possible plume to the NE, suggesting a disturbed morphology.

01098-2754 The H α -NII blend is marginally resolved in this object, with H α being the dominant line. This suggests an HII region-like spectrum. SII is also clearly detected.

Imaging shows this ULIRG to be a complex system involving two nuclei and a tail to the E. The separation of the nuclei is about 6 arcseconds.

02226-1658 A line is detected at 8087\AA which we identify as the H α -NII blend. The only other interpretation for this line is MgII at $z=1.89$, which would make this an unusually luminous galaxy. We do not consider this a reasonable interpretation, and favour the lower redshift value. This adopted redshift, however, must be regarded as tentative.

The image of this ULIRG is undistinguished.

03156-1706 This object has a strong broad H α line with a velocity width of $\sim 4000 \text{ kms}^{-1}$. H β , with a similar width, is also detected, as is OIII5007/4959. The broad-line nature of this object leads us to classify it as a rare IR luminous quasar. Structure in the spectrum redward of OIII might be due to FeII emission which is often associated with strong far-IR emission in quasars (Lipari et al. 1993, 1994). The object also appears to have an unusually blue continuum.

Imaging shows that this object probably lies in a rich group or galaxy cluster. We do not detect signs of interaction though. An alternative interpretation is that this object is being gravitationally lensed by a foreground group or cluster.

21498-2636 H α is detected in this object, as is SII, though only weakly. An unambiguous assessment of the nature of its spectrum is not possible since the H α detection is not of sufficient signal-to-noise, but it is most likely to be HII region-like.

The image of this galaxy shows two plumes or tails to the NW and SW, suggesting a disturbed morphology. A possible interaction companion lies 6 arcseconds to the SE.

23169-0818 The H α -NII blend is marginally resolved here, and the SII and OI lines are also detected. The relative strengths of H α and NII suggest an HII region-like spectrum.

This ULIRG has a second nucleus or plume to the NW. The separation between the main and putative second nucleus is ~ 3 arcseconds.

23569-0341 Two lines are detected in this object that match with H α -NII and SII at a redshift of 0.304. The H α -NII lines are not strong enough to draw any conclusions about the nature of the spectrum.

Figure 1. Spectra of the Newly Identified ULIRGs

Wavelength is given in Å, while the flux scale is arbitrary. See Table 1 and Section 4.1 for details of the individual objects.

The image of this object is an undistinguished, marginally resolved galaxy.

5 DISCUSSION

5.1 The ULIRG Population

The present work adds 11 ULIRGs, of which 3 are provisional identifications, to the large ULIRG survey that we

Figure 2. Images of the Newly Identified ULIRGs

All images are 1x1 arcminute in size, and were taken in the R band. Typical integration times are 120s. Seeing was between 1 and 2 arcseconds. See Table 1 and Section 4.1 for details of individual objects.

have undertaken, bringing the total number of ULIRGs in the survey to 102. The highest redshift in the survey is now 0.44, and a substantial number of objects have been added between $z=0.3$ and 0.4. For those objects where we can attempt some spectral classification, we find that 3/7 have high ionisation spectra. These include one object that appears to be a new IR luminous quasar, another with a somewhat broad $H\alpha$ line, and another with strong NII and OIII emission. This is consistent with the result in Paper 1 that at least 35% of ULIRGs contain AGNs. Morphological studies of the acquisition images show that five of the eight objects (62%), where we have deep enough images to attempt a classification, are in disturbed systems. This compares with a value of 91% found by Clements et al. (1996b) and Murphy et al. (1996) in larger, deeper imaging studies. However, it has been shown that signs of interaction can often be missed in shallow images (Clements & Baker, 1996), so 5/8 should probably be regarded as a lower limit.

03156-1706, the broad line IR luminous quasar that we have discovered, is probably the most interesting object in the present paper. It is one of only a small number of IRAS selected quasars and is only the third confirmed broad-line object in our ULIRG survey (the others are Mrk1014 and 00275-2859). The possible detection of FeII emission is of particular interest since it has been claimed that FeII emission is possibly associated with young quasars, just emerging from a dust obscured ULIRG phase (Lipari et al, 1993, 1994). This object also has quite a warm $25\mu\text{m}$ -to- $60\mu\text{m}$ colour ($f_{25}/f_{60} = 0.39$), making it similar to the Lipari et al. FeII emitters. High signal-to-noise and better resolution spectra will be needed to confirm an FeII detection, but it is interesting to note that the Fe II emission is probably somewhat weaker than in the strong/extreme Fe II emitters discussed by Lipari et al. It thus might be a transition object in a post-starburst phase where the AGN is making a significant contribution to the far-IR luminosity.

5.2 Status of the ULIRG Survey

We have now observed all but 89 objects in our original sample of 479 sources so there is an overall observational completeness of 81%. Redshifts have been obtained for 329 objects, while ten of these objects have turned out to be stars, giving a redshift completeness of 70%, compared with 60% in Paper 1. Figure 3 shows the present cumulative completeness as a function of loudness. We also show in Figure 4 the fraction of ULIRGs among objects with measured redshifts as a function of IR loudness (R_1 and R_2). This demonstrates the effectiveness of our selection technique. We can also use this diagram to predict the number and IR loudness of the ULIRGs currently awaiting discovery in our candidate list. This suggests that we have about 40 ULIRGs still to uncover, the vast majority of which will have $R_1 > 50$.

In the present catalogue there are now 30 objects that we classify as 'dull'. These are candidate identifications for the IRAS sources whose spectra show a strongly detected continuum but no emission lines. 14 objects previously classified as dull now have redshifts. Most of these have weak line/continuum ratios, though a few are identified with objects other than the highest likelihood identification. They do not appear to be a cohesive class which might bias es-

Figure 3. Completeness as a Cumulative Function of IR Loudness

The upper lines show observational completeness for objects having an infrared loudness greater than the value indicated on the x axis, while the lower lines show the same for redshift completeness. Solid lines are for R_1 , dotted for R_2 . [NOTE: The completeness diagram shown in Paper 1 is misleading. The present diagram is a better representation of the actual completeness].

Figure 4. Fraction of ULIRGs as Function of IR Loudness

The lines give the fraction of ULIRGs among galaxies with a measured redshift. The low values shown for low loudness values demonstrates the effectiveness of our selection technique. The solid line gives values for R_1 , the dotted line for R_2 . We find that R_1 , our primary selection parameter, is somewhat better at selecting ULIRGs than R_2 .

timates of luminosity function evolution if they are not included.

6 CONCLUSIONS

Continuing observations to identify ULIRGs in our large area survey have identified 8 clear new ULIRGs and 3 further probable ULIRGs whose redshifts are in need of confirmation. One of these objects is a new IR luminous quasar, while another increases the maximum redshift in the survey to 0.44. The survey is now $\sim 70\%$ complete in redshift identifications. The loudness selection criteria seem to be working very well, especially R_1 , and we predict that there are about 40 more ULIRGs to find in this survey, most of which will have $R_1 > 50$.

ACKNOWLEDGMENTS

It is a pleasure to thank the support staff at ESO for their help with the observations. This research has made use of the NASA/IPAC Extragalactic Database (NED) which is operated by the Jet Propulsion Laboratory, California Institute of Technology, under contract with the National Aeronautics and Space Administration. DLC is supported by an ESO Fellowship and by the EC TMR Network programme, FMRX-CT96-0068., WS and RGM are supported by Royal Society Fellowships. We would like to thank the anonymous referee for helpful comments.

REFERENCES

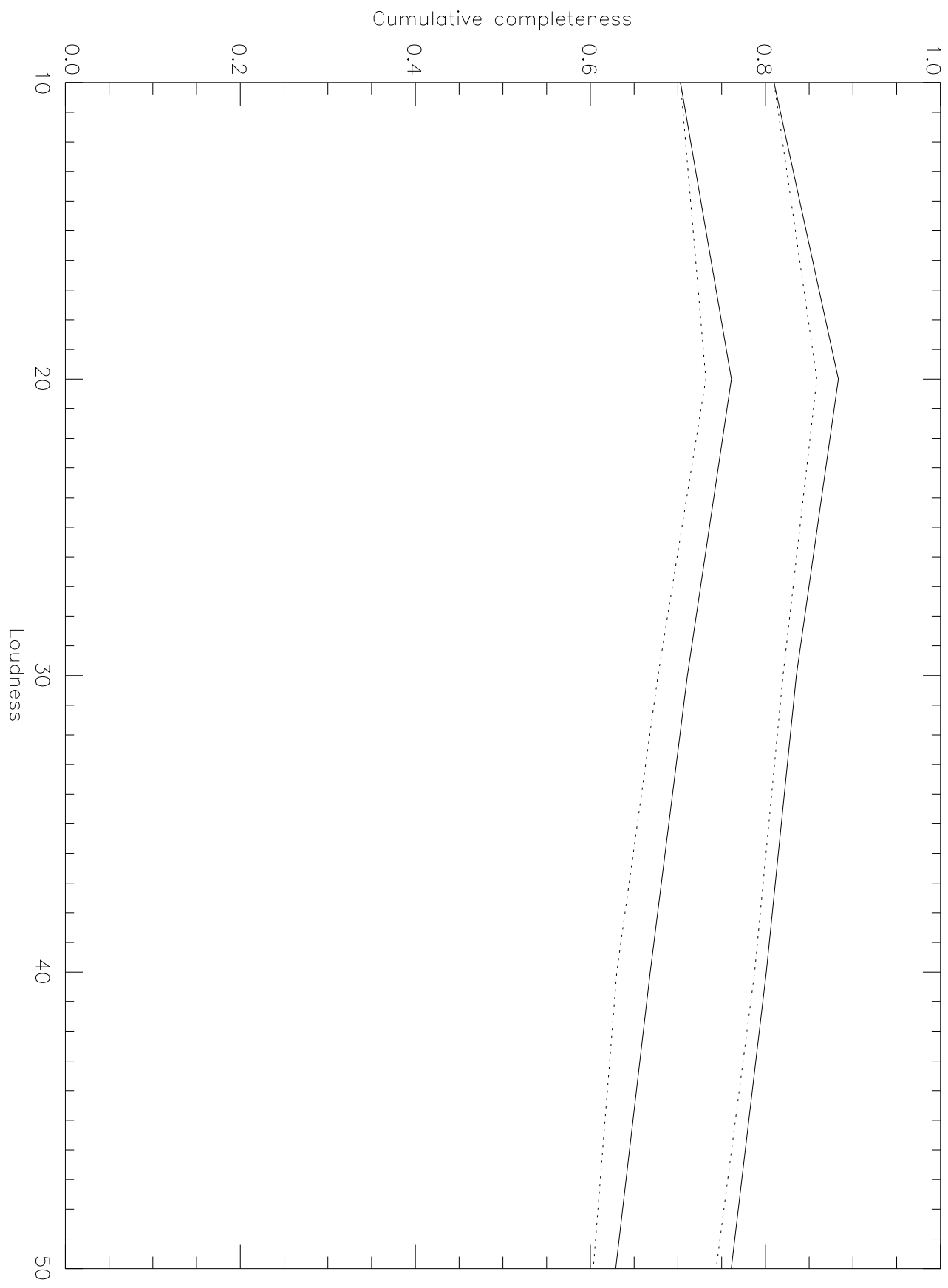
- Boyle, B.J., Shanks, T., Peterson, B.A., 1988, MNRAS, 235, 935
 Broadhurst, T.J., Ellis, R.S., Shanks, T., 1988, MNRAS, 235, 827
 Clements D.L., Sutherland W.J., Saunders W., McMahon R.G., Maddox S., Lawrence A., Efstathiou G.P., Rowan-Robinson M., 1996a, MNRAS, 279, 459, Paper 1
 Clements D.L., Sutherland W.J., Saunders W., McMahon R.G., 1996b, MNRAS, 279, 477
 Clements, D.L., Baker, A.C., 1996, A&A, 314, L5
 Colless, M.M., Ellis, R.S., Taylor, K., Hook, R.N., 1990, MNRAS, 244, 408
 Dunlop, J.S., Peacock, J.A., 1990, MNRAS, 247, 19
 Fisher, K.B., Huchra, J.P., Strauss, M.A., Davis, M., Yahil, A., Schepgel, D., ApJS, 100, 69
 Kim, D-C., Sanders, D.B., Veilleux, S., Mazzarella, J.M., Soifer, B.T., 1995, ApJS, 98, 128
 Lipari S., Terlevich, R., Macchetto, F., 1993, ApJ., 406, 451
 Lipari S., 1994, ApJ., 436, 102
 Lonsdale, C.J., Diamond, P.J., Smith, H.E., Lonsdale, C.J., 1998, ApJ., 493, L13
 Lutz, D., et al., 1996, A&A, 315, L137
 Melnick, J., 1995, The EFOSC1 Operating Manual Update, published by ESO
 Moshir M. et al., 1992, The IRAS Faint Source Survey, published by IPAC.
 Murphy, T.W., Armus, L., Matthews, K., Soifer, B.T., Mazzarella, J.M., Shupe, D.L., Strauss, M.A., Neugebauer, G., 1996, AJ., 111, 1025
 Rowan-Robinson, M., 1995, MNRAS, 272, 737
 Sanders D.B., Soifer B.T., Elias J.H., Madore B.F., Matthews K., Neugebauer G., Scoville N.Z., 1988, ApJ, 325, 74
 Sanders D.B., Phinney E.S., Neugebauer G., Soifer B.T., Matthews K., 1989, ApJ, 347, 29
 Sanders, D.B., Mirabel, I.F., 1996, ARAA, 34, 749
 Saunders, W., Rowan-Robinson, M., Lawrence, A., Efstathiou, G., Kaiser, N., Ellis, R.S., Frenk, C.S., 1990, MNRAS, 242, 318
 Sutherland, W.J., Saunders, W., 1992, MNRAS 259, 413
 Veilleux, S., Kim, D-C., Sanders, D.B., Mazzarella, J.M., Soifer, B.T., 1995, ApJS, 98, 171
 Wright, G.S., Joseph, R.D., Mickle, W.P.S., Nat, 309, 430

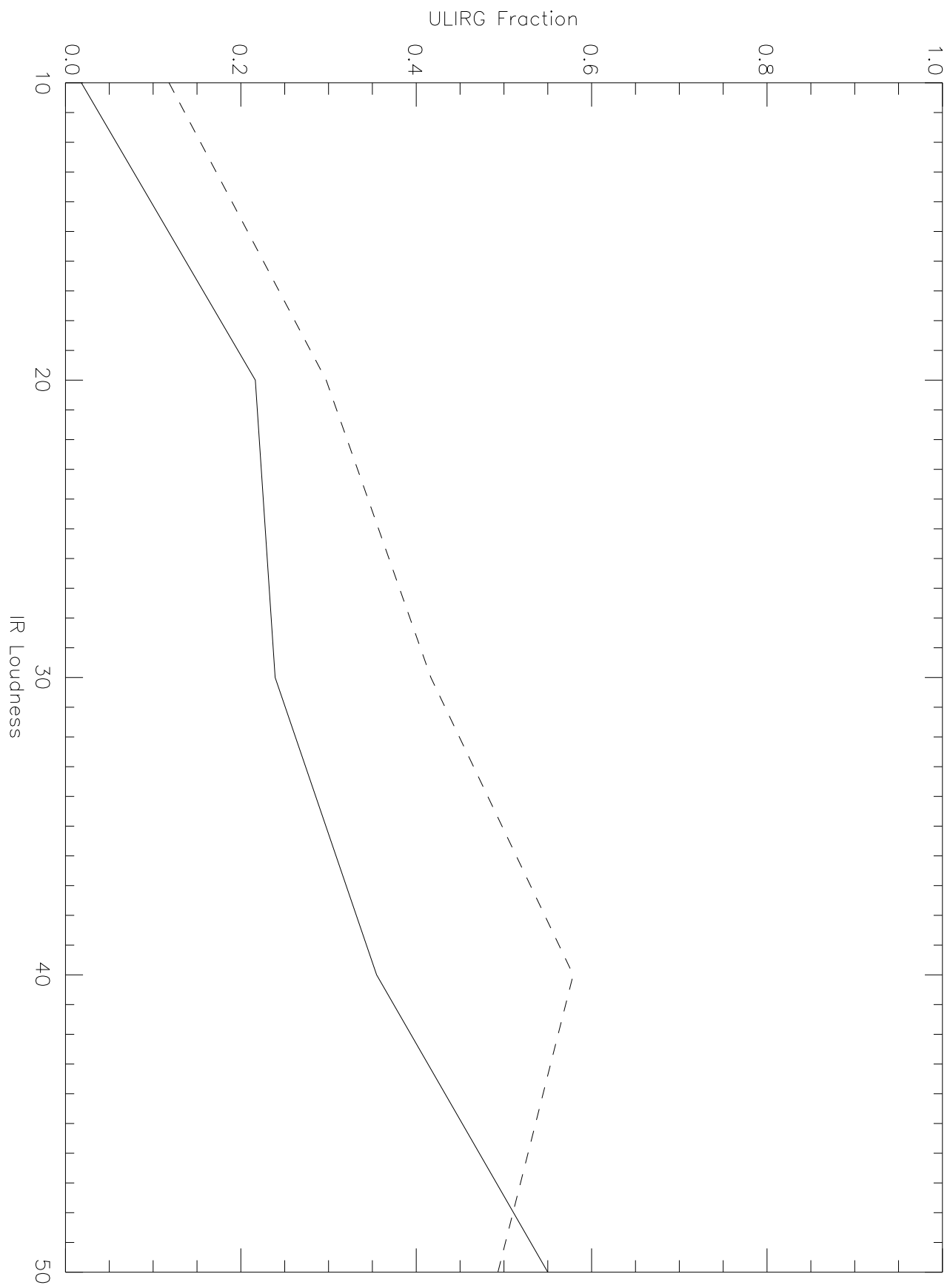
Appendix A

We here present the new redshifts obtained for non-ultraluminous objects in the course of this survey.

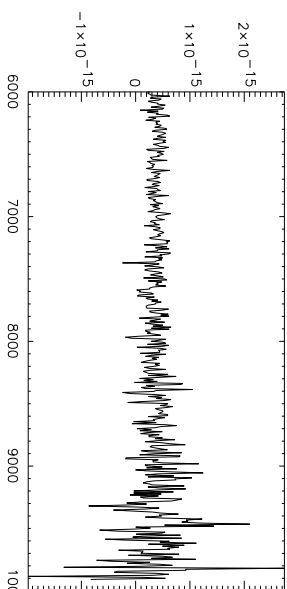
Name	RA(1950)	DEC(1950)	$f_{60}(\text{Jy})$	z	$\log(L_{60}/L_{\odot})$
00016-3056	00 01 39.70	-30 56 49.2	0.79	0.065	10.68
00107-1850	00 10 46.83	-18 50 48.8	0.31	0.096	10.62
00113-2830	00 11 22.97	-28 30 59.4	0.37	0.179	11.25
00264-2348	00 26 28.79	-23 48 19.2	0.31	0.065	10.28
00353-0641	00 35 21.64	-06 41 15.9	4.78	0.023	10.55
00363-1732	00 36 20.36	-17 32 59.2	0.41	0.147	11.12
00395-1743	00 39 35.45	-17 43 18.1	0.69	0.136	11.28
00408-0833	00 40 51.20	-08 33 12.0	0.47	0.086	10.71
00472+0010	00 47 12.42	+00 10 51.1	0.40	0.120	10.93
00566-1456	00 56 41.54	-14 56 38.5	0.53	0.05	10.28
01212-0347	01 21 15.55	-03 47 38.3	0.61	0.090	10.86
01290-1557	01 29 02.92	-15 57 06.7	0.45	0.104	10.85
01359-0051	01 35 59.52	-00 51 35.9	0.34	0.120	10.86
01394-0839	01 39 29.30	-08 39 47.2	0.36	0.145	11.05
01420-2033	01 42 04.73	-20 33 56.7	0.53	0.091	10.81
01506-2046	01 50 41.80	-20 46 30.6	0.46	0.109	10.91
01573-1722	01 57 18.70	-17 22 54.0	0.35	0.153	11.09
02059-1145	02 05 59.15	-11 45 46.4	0.49	0.154	11.24
02105-1954	02 10 35.30	-19 54 37.0	0.38	0.086	10.61
02150-2545	02 15 00.55	-25 45 20.2	0.33	0.218	11.38
02259-2122	02 25 59.00	-21 22 18.4	0.42	0.174	11.28
03314-2643	03 31 24.92	-26 43 35.4	1.84	0.084	11.28
03355-3113	03 35 43.36	-31 13 38.7	0.46	0.128	11.05
21499-2839	21 49 56.05	-28 39 31.1	0.32	0.135	10.94
22012-2144	22 01 15.00	-21 44 31.9	0.51	0.068	10.53
22028-1815	22 02 52.28	-18 15 22.5	0.45	0.162	11.25
22049-2833	22 04 56.23	-28 33 05.3	0.38	0.176	11.25
22205-2941	22 20 30.70	-29 41 20.1	0.61	0.122	11.13
22222-0846	22 22 12.39	-08 46 20.0	0.35	0.123	10.89
22586+0205	22 58 44.98	+02 05 17.8	0.34	0.042	9.93
23003-2625	23 00 23.51	-26 25 43.5	0.51	0.088	10.76
23033-3134	23 03 21.48	-31 34 07.4	0.32	0.192	11.26
23131-0403	23 13 06.70	-04 03 31.0	0.32	0.122	10.85
23131-2854	23 13 07.30	-28 54 57.0	0.38	0.185	11.30
23279-2224	23 27 56.04	-22 24 18.0	0.31	0.175	11.16
23390-0217	23 39 02.10	-02 17 44.9	0.30	0.167	11.10
23394-0502	23 39 24.01	-05 02 06.0	0.36	0.08	10.53
23575-2352	23 57 31.63	-23 52 24.9	0.31	0.100	10.66
23584-2704	23 58 29.38	-27 04 53.5	0.33	0.137	10.97
23598-1327	23 59 52.90	-13 27 23.0	0.31	0.181	11.19

Table 2. Data for non-ULIRGs discovered in the survey

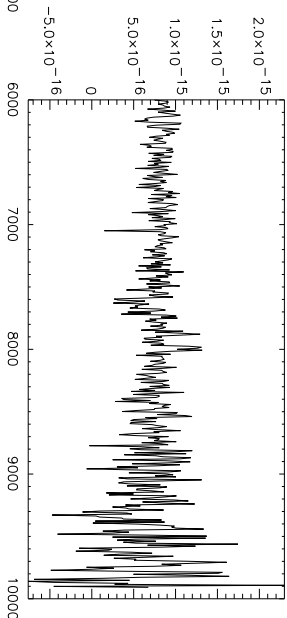




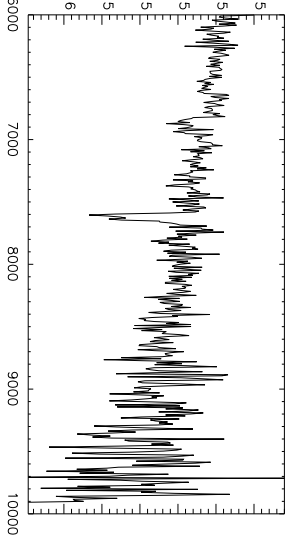
00029-1424



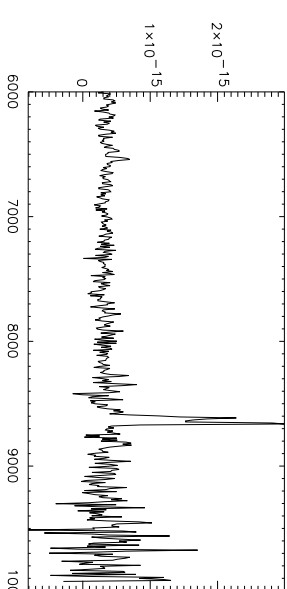
00285-3140



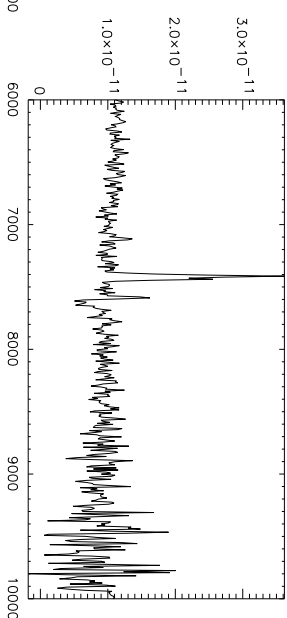
00366-0503



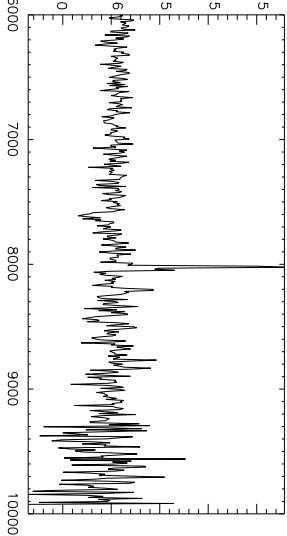
00415-0737



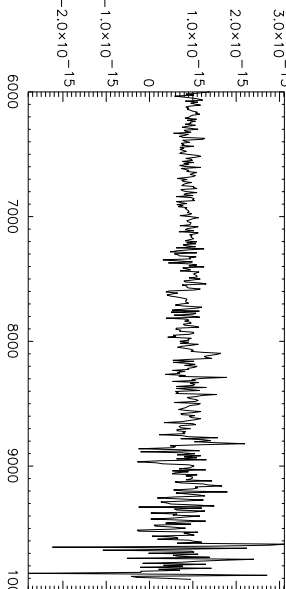
00482-2720



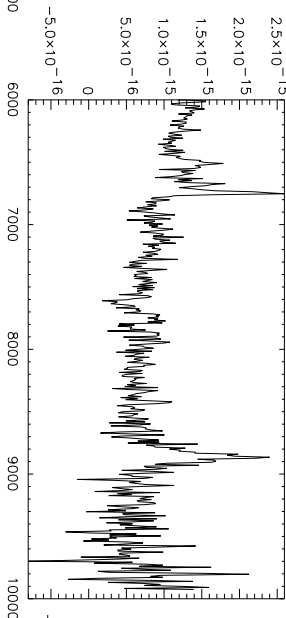
01098-2754



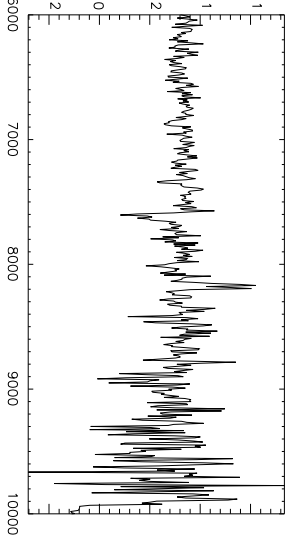
02226-1658



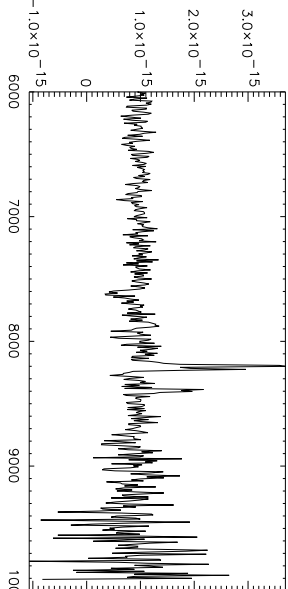
03156-1706



21498-2636



23169-0818



23569-0341

